4th Joint US-Korea Workshop on Mesoscale Observation, Data Assimilation and Modeling for Severe Weather. 13-15 February 2006, Seoul, Korea.

Data Assimilation and Prediction at the Convective Scale: Recent Progresses

Ming Xue
Center for Analysis and Prediction of Storms and School of Meteorology
University of Oklahoma, Norman Oklahoma 73019, USA
mxue@ou.edu

1. Introduction

In this paper, we briefly present some recent results of initialization and prediction of convective-scale weather systems using a high-resolution numerical model and its data assimilation systems. For cases with pre-existing storms, the WSR-88D radar data are assimilated, at 5 to 15 minute intervals, over a typically one-hour assimilation window, using three-dimensional variational (3DVAR) method plus a cloud analysis scheme (Hu 2005; Hu and Xue 2006; Hu et al. 2006a; Hu et al. 2006b), or the ensemble Kalman filter (EnKF) method (Tong and Xue 2005; Xue et al. 2006). Predictions of individual thunderstorms for up to three hours are performed and directly compared to radar measurements. Also discussed are a study on the detailed processes responsible for the initiation of convection along a dryline (Xue and Martin 2006a, b) and new conceptual model for the processes.

2. Initialization of convective storms using 3DVAR and cloud analysis of radar data

In the studies of Hu et al. (2006a,b) and Hu and Xue (2006), a 3DVAR-cloud analysis combination is used and shown to be efficient and effective for initializing convective storms using radar data. Typically, rapid update cycles at 5 to 15 minutes intervals are used to achieve the best results (Hu and Xue 2006). Fig. 1 shows the predicted radar echoes over a 2.5-hour period for a supercell storm at 3 km resolution (Hu and Xue 2006). The direction and characteristics of the storm were well predicted by the model. Using initial conditions thus obtained, but interpolated to a 100 m resolution grid, a tornado is obtained in the forecast that reaches an F2 intensity (Fig. 2). This predicted tornado is within 10 km of the actual F3-intensity tornado observed on May 8, 2003 near Oklahoma City and presents the first time ever that a tornado is predicted by a numerical model initialized using real radar data (Hu 2005).

3. Ensemble Kalman filter method for radar data assimilation

The ensemble Kalman filter (EnKF) method has shown great promises in a number of recent studies that use simulated radar data (Snyder and Zhang 2003; Zhang et al. 2004; Tong and Xue 2005; Xue et al. 2005a). The EnKF method appears to be more attractive for convective scale applications due to high degrees of nonlinearity in both model physics and observation operators at such scales. Fritsch and Carbone (2004) suggested that EnKF may be the most powerful tool for DA for summer time precipitation and Lorenc (2003) also suggested a potentially larger role of EnKF at the mesoscale.

Tong and Xue (2005) show that the mixing ratios of all species associated with a 5-class (cloud, rain, ice, snow and hail) microphysics scheme can be accurately analyzed/retrieved using an EnKF algorithm from simulated radar (radial velocity and reflectivity) data.

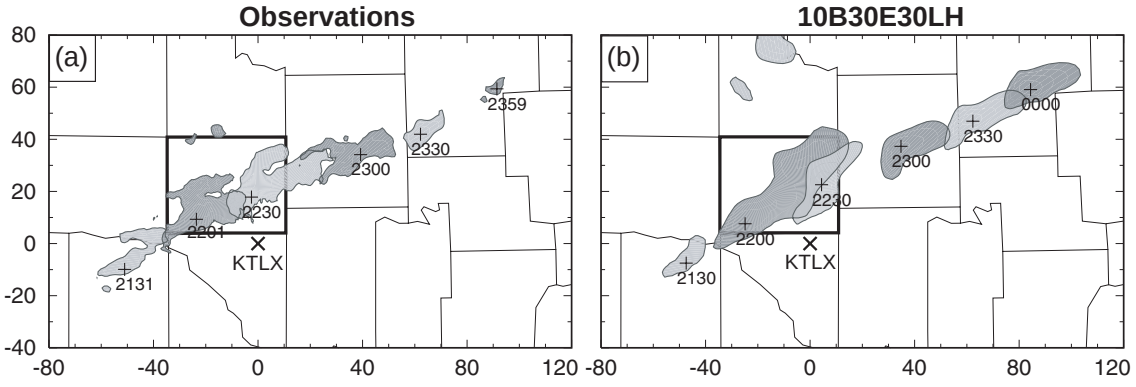

Fig. 1. Regions of radar echoes exceeding 35 dBZ as observed by KTLX radar (a) at the 1.45º elevation at 30-minute intervals from 2101 to 2359, of 8 May 2003. The right panel contains the model predicted echoes mapped to the same radar elevation.

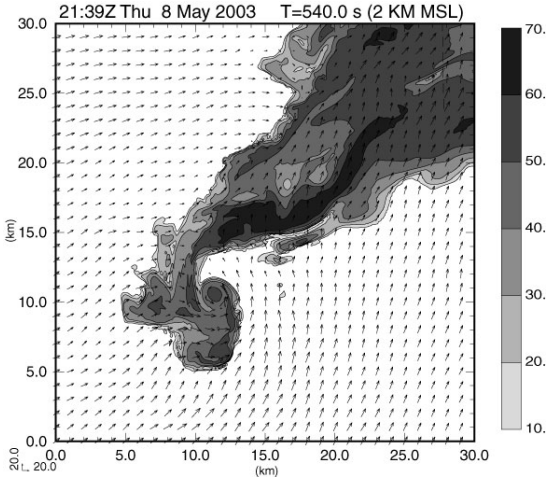

Fig. 2. Predicted reflectivity and wind fields at 2 km MSL 9 minutes into the 100 m forecast. Domain is 30 by 30 km2. A tornado is clearly indicated by the hook echo that contains reflectivity spirals into the circulation center.

Studies with EnKF and real data are so far limited, however. For a global model, Houtekamer et al. (2005) compared the performance of an EnKF system with an operational 3DVAR system and found generally comparable results. The presence and treatment of model errors with real data are believed to be the most important issues. For radar DA, Dowell et al. (2004) is currently the only published work that deals with real data; the paper contains no prediction component, however. A similar level of accuracy for the analysis is obtained by our group, assimilating real radial velocity (V_r) and radar reflectivity (Z) data from a WSR-88D radar at Oklahoma City (KTLX) for a tornadic supercell case (Xue et al. 2005b). One km horizontal resolution and 40 ensemble members were used in our case.

Fig. 3 shows the analyzed reflectivity at the end of a 1-hour assimilation period, interpolated to the 1.25º elevation of KTLX radar as compared to the observation. The analyzed storm exhibits typical supercell structures, including low-level hook echo, mid-level mesocyclone, intense updraft, as well as low-level gust front and convergence center (not shown). The ensuing forecast starting from the analysis is not very satisfactory, however. The predicted storm propagates too fast during a 1.5 hour period, and there is indication that both analyzed and forecast cold pools are too strong. Too strong cold outflow also developed during the assimilation period of Dowell et al. (2004). Microphysics parameterization is likely a major source of error in such cases. We found through a large set of experiments that the maximum temperature deficit within the cold pool of simulated supercell storms can change from a few degrees to nearly twenty degrees, by simply changing the intercept parameters of rain, snow and/or hail within their observed ranges. A 10-ice single or double-moment microphysics and a sophisticated three-moment microphysics scheme are being implemented in our model, and will be used for these studies.

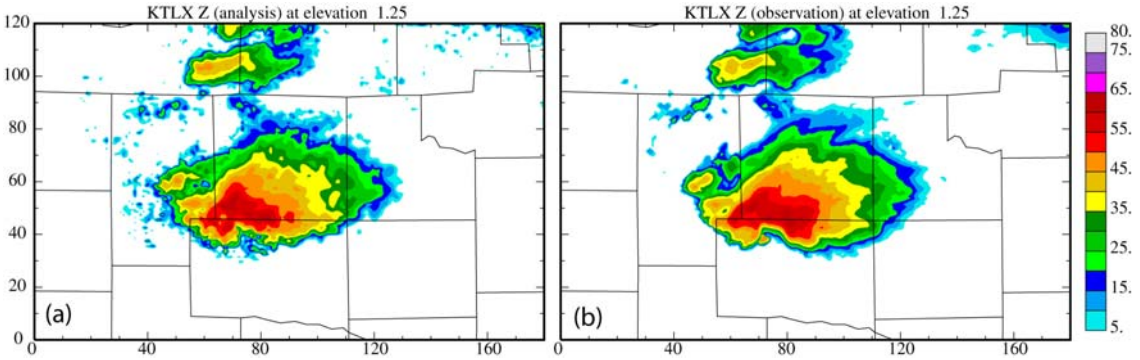

Fig. 3. The analyzed reflectivity field at the 1.25º elevation (a) as compared to the corresponding observed reflectivity (b), at the end of an hour-long assimilation period, for the May 29-30 2004 north Oklahoma City tornadic thunderstorm. OKC WSR-88D radar radial velocity and reflectivity data were assimilated.

4. Convective initiation

The prediction of convective storms before they form poses a different problem than initializing a pre-existing storm that can be captured by precipitation-mode radars. The convective initiation processes of the May 24, 2002 case during IHOP_2002 (Weckwerth and Parsons 2005) are studied in depth by Xue and Martin (2006a; 2006b), through high-resolution (1 km) numerical simulations. By assimilating high-density surface networks and other special observations from IHOP, three series of convective cells initiated at specific locations of the dryline were accurately predicted to within 20 min and 25 km of the true cells. The model also correctly predicted the lack of initiation of convection at the dryline-cold front triple point to the north, on which a large array of instruments were focused on that day. For the first

time, the exact process by which boundary-layer eddies and horizontal convective rolls interact with the dryline convergence line to determine the exact locations of cell initiation were simulated for a real case. Many simulated features at various scales were found to agree well with new (IHOP) and past observational data. Based on these simulations, a new conceptual model for dryline convective initiation is proposed, which is shown in Fig. 4. The sensitivity of precipitation forecast to the initial boundary layer moisture as well as to other fields is studied for the same case by Martin and Xue (2006) using a novel very-large-ensemble technique. The method has the advantage of being able to deal with nonlinear responses. Very large sensitivities of certain precipitation to localized low-level moisture are found in the study.

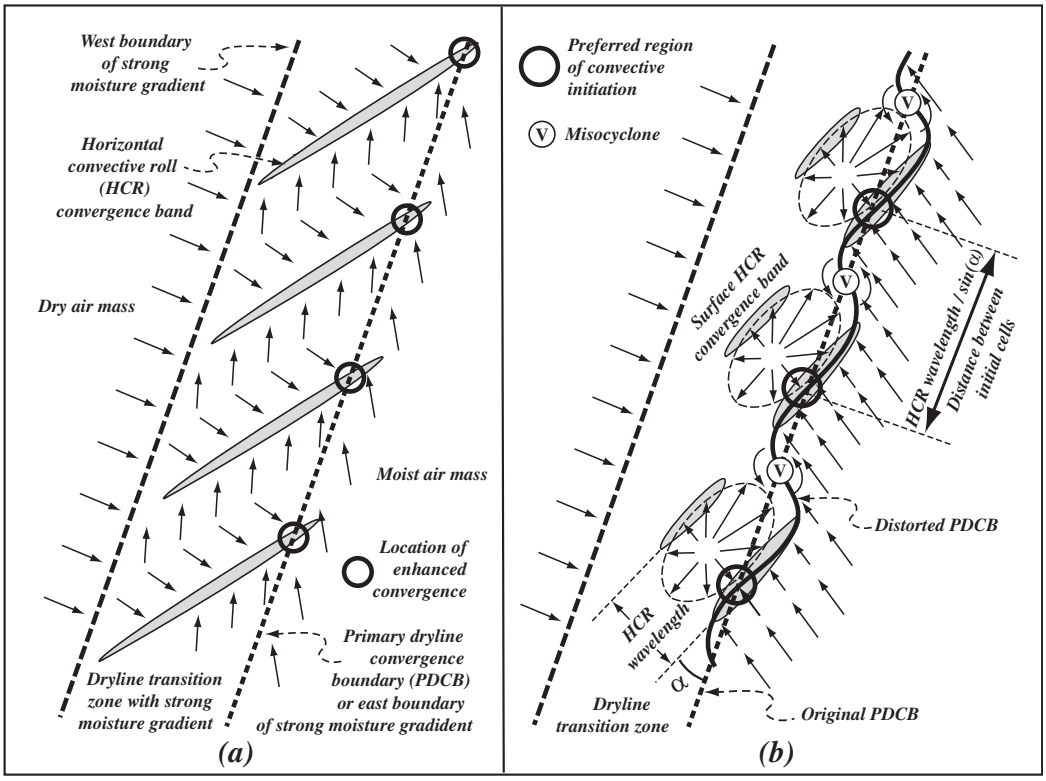

Fig. 4. A conceptual model of dryline convective initiation due to the interaction of the primary dryline convergence boundary (PDCB) with the evolving horizontal convective rolls (HCRs) that originate at and on the west side of the PDCB and are aligned at an acute angle, α, with the dryline. The PDCB is the boundary between the southerly to southeasterly moist flow, and the drier generally westerly flow in the dryline transition zone, where a strong moist gradient is found. The PDCB undistorted by the HCR circulation is marked by the thick, straight, short-dashed line. The thick, straight, long-dashed line marks the location of the western boundary of the dryline transition zone, toward the west of which the air is exclusively from the dry high plateau to the west with a specific humidity of few grams per kilogram. Panel (a) shows the earlier stage of HCR development when the HCRs are quasi-two-dimensional and the roll circulations result in surface divergence flow and convergence bands (shaded gray) between the opposing roll circulations. The background southwesterly wind in the transition zone causes the surface divergence flow of the rolls to point in the downwind direction. The rolls are aligned in the direction of the mean low-level vertical shear vector and the northeastern ends of the convergence bands intersect the PDCB, creating localized convergence maxima. Panel (b) shows the low-level flow at the mature stage of HCR development, about 1-2 hours after panel (a), when significant cellular structures develop with the rolls and the convergence bands becoming segmented and shorter but more intense. The convergence bands protrude further into the moist air mass across the original PDCB and distort the PDCB into a wavy pattern. The divergence flow between the convergence bands develops into asymmetric elliptic patterns, with the northeastward wind components being stronger due to downward transport of southwesterly momentum and due to the original background flow in the same direction. The mesoscale convergence along the dryline is enhanced by the elevated heating to the west hence by the increased solenoidal forcing. It narrows the dryline transition zone, turns the HCRs into a more north-south orientation. The easterly component of the moist flow is increased, which, together with HCR divergence

flow, creates convergence maxima along the PDCB, at locations marked by thick circles, where convective initiation is preferred. Such locations are also roughly where HCRs intersect the original PDCB and the distance between such preferred locations is roughly equal to the HCR wavelength divided by sin(α). When the initiated clouds move along the HCR convergence bands, they develop into deeper clouds faster and have a much better chance of growing into a full intensity convective storm. When older cells that are initiated at the persistent maximum low-level convergence forcing move away, new cells tend to form at the same location, resulting in a series of cells. The thin circles enclosing 'V' indicate locations of vorticity maxima (or misocyclones) along the PDCB. Misocyclones usually do not co-locate with maximum surface convergence but their circulation can enhance convergence to their south and north, and non-supercell tornadoes can develop when their vertical vorticity is stretched by cumulus congestus clouds that move over them.

5. Summary

Several recent studies on the initialization and prediction of convective weather systems are discussed. These studies shows great promises of explicit prediction of convective systems, using high-resolution NWP models and advanced data assimilation techniques that include high-resolution in-situ and remotely sensed data. With proper initiation of tornadic thunderstorms, a successful prediction of an F-2 intensity tornado is obtained for the first time using a full physics numerical model. More details on the results can be found in the referenced papers and will be discussed at the workshop.

References

Dowell, D., F. Zhang, L. J. Wicker, C. Snyder, and N. A. Crook, 2004: Wind and temperature retrievals in the 17 May 1981 Arcadia, Oklahoma supercell: Ensemble Kalman filter experiments. *Mon. Wea. Rev.*, **132,** 1982-2005.

Fritsch, J. M. and R. E. Carbone, 2004: Improving quantitative precipitation forecasts in the warm season: A USWRP research and development strategy. *Bull. Amer. Meteor. Soc.*, **85,** 955-965.

Houtekamer, P. L., H. L. Mitchell, G. Pellerin, M. Buehner, M. Charron, L. Spacek, and B. Hansen, 2005: Atmospheric data assimilation with an ensemble Kalman filter: Results with real observations. *Mon. Wea. Rev.*, **133,** 604-620.

Hu, M., 2005: 3DVAR and cloud analysis with SWR-88D level-II data for the prediction of tornadic thunderstorms, School of Meteorology, University of Oklahoma, 217.

Hu, M. and M. Xue, 2006: Impact of configurations of rapid intermittent assimilation of WSR-88D radar data for the 8 May 2003 Oklahoma City tornadic thunderstorm case. *Mon. Wea. Rev.***,** Conditionally accepted.

Hu, M., M. Xue, and K. Brewster, 2006a: 3DVAR and Cloud analysis with WSR-88D Level-II Data for the Prediction of Fort Worth Tornadic Thunderstorms. Part I: Cloud analysis and its impact. *Mon. Wea. Rev.*, **134,** 675-698.

Hu, M., M. Xue, J. Gao, and K. Brewster, 2006b: 3DVAR and Cloud analysis with WSR-88D Level-II Data for the Prediction of Fort Worth Tornadic Thunderstorms. Part II: Impact of radial velocity analysis via 3DVAR. *Mon. Wea. Rev.*, **134,** 699-721.

Lorenc, A., 2003: The potential of the ensemble Kalman filter for NWP - a comparison with 4D-Var. *Quart. J. Roy. Meteor. Soc.*, **129,** 3183-3204.

Martin, W. J. and M. Xue, 2006: Initial condition sensitivity analysis of a mesoscale forecast using very-large ensembles. *Mon. Wea. Rev.*, **134,** 192–207.

Snyder, C. and F. Zhang, 2003: Assimilation of simulated Doppler radar observations with an ensemble Kalman filter. *Mon. Wea. Rev.*, **131,** 1663-1677.

Tong, M. and M. Xue, 2005: Ensemble Kalman filter assimilation of Doppler radar data with a compressible nonhydrostatic model: OSS Experiments. *Mon. Wea. Rev.*, **133,** 1789-1807.

Weckwerth, T. M. and D. B. Parsons, 2005: Outstanding issues in convective initiation: Motivation for IHOP_2002. *Mon. Wea. Rev.***,** Accepted.

Xue, M. and W. J. Martin, 2006a: A high-resolution modeling study of the 24 May 2002 case during IHOP. Part I: Numerical simulation and general evolution of the dryline and convection. *Mon. Wea. Rev.*, **134,** 149–171.

Xue, M. and W. J. Martin, 2006b: A high-resolution modeling study of the 24 May 2002 case during IHOP. Part II: Horizontal convective rolls and convective initiation. *Mon. Wea. Rev.*, **134,** 172–191.

Xue, M., M. Tong, and K. K. Droegemeier, 2005a: An OSSE framework based on the ensemble square-root Kalman filter for evaluating impact of data from radar networks on thunderstorm analysis and forecast. *J. Atmos. Ocean Tech.***,** Accepted.

Xue, M., M. Tong, and M. Hu, 2005b: Assimilation of Radar Data for Thunderstorm Prediction with Ensemble Kalman Filter Method. *Abstract, 4th WMO Int. Symp. Assimilation Obs. Meteor. Ocean.*, Prague, Czech Republic.

Xue, M., M. Tong, and K. K. Droegemeier, 2006: An OSSE framework based on the ensemble square-root Kalman filter for evaluating impact of data from radar networks on thunderstorm analysis and forecast. *J. Atmos. Ocean Tech.*, **23,** 46–66.

Zhang, F., C. Snyder, and J. Sun, 2004: Impacts of initial estimate and observations on the convective-scale data assimilation with an ensemble Kalman filter. *Mon. Wea. Rev.*, **132,** 1238-1253.